Molecular Crystals and Liquid Crystals

Publication details, including instructions for authors and subscription information:
http://www.tandfonline.com/loi/gmcl20

Molecular Organization of Preorganized S-Shaped Oligomers in the Liquid Crystalline Phases

Yoshihiro Nagashima [a], Fumitaka Ogasawara [a b], Jun Yamamoto [c], Yoichi Takanishi [c] & Atsushi Yoshizawa [a]

[a] Department of Frontier Materials Chemistry, Graduate School of Science and Technology, Hirosaki University, Hirosaki, Japan

[b] Tohoku Chemical Corporation, Hirosaki, Japan

[c] Department of Physics, Graduate School of Science, Kyoto University, Kyoto, Japan

Version of record first published: 05 Oct 2009

To cite this article: Yoshihiro Nagashima, Fumitaka Ogasawara, Jun Yamamoto, Yoichi Takanishi & Atsushi Yoshizawa (2009): Molecular Organization of Preorganized S-Shaped Oligomers in the Liquid Crystalline Phases, Molecular Crystals and Liquid Crystals, 509:1, 233/[975]-244/[986]

To link to this article: http://dx.doi.org/10.1080/15421400903054527

Mol. Cryst. Liq. Cryst., Vol. 509, pp. 233/[975]–244/[986], 2009

ISSN: 1542-1406 print/1563-5287 online
DOI: 10.1080/15421400903054527

Molecular Organization of Preorganized S-Shaped Oligomers in the Liquid Crystalline Phases

Yoshihiro Nagashima[1], Fumitaka Ogasawara[1,2], Jun Yamamoto[3], Yoichi Takanishi[3], and Atsushi Yoshizawa[1]
[1]Department of Frontier Materials Chemistry, Graduate School of Science and Technology, Hirosaki University, Hirosaki, Japan
[2]Tohoku Chemical Corporation, Hirosaki, Japan
[3]Department of Physics, Graduate School of Science, Kyoto University, Kyoto, Japan

*We prepared a homologous series of S-shaped oligomers, 4,4′-bis(ω-(2-(ω-(4-(cyanophenyl)phenyloxy)alkyloxy)phenyloxy)alkyloxy)biphenyl [***I-(m,n)***], and investigated effects of the spacer length on the phase transition behavior.* **I-(7,7), I-(8,8), I-(9,9)** *and* **I-(7,9)** *showed nematic (N) and smectic A (SmA) phases, whereas* **I-(6,6)** *and* **I-(6,9)** *showed only an N phase. The melting behavior was found to depend on the parity of the spacer (***m***). The liquid-crystalline phases of* **I-(8,8)** *and* **I-(6,9)** *are monotropic, however, those of* **I-(9,9)** *and* **I-(7,9)** *are enantiotropic. X-ray diffraction measurements of* **I-(7,7), I-(8,8)** *and* **I-(7,9)** *indicate that the S-shaped oligomers exist as a close-packed structure in the monolayer SmA phase.*

Keywords: liquid crystals; oligomer; phase transition; S shape

1. INTRODUCTION

Oligomeric liquid crystals are current topics in the design of new liquid crystalline materials because of their abilities to form supramolecular assemblies [1]. In addition, molecular topology has attracted much attraction as the origin for producing novel self-organizing systems. One of the initial investigation for oligomeric liquid crystals was dimer in which mesogenic moieties are connected *via* a flexible alkyl spacer. The well-known series of symmetric liquid-crystalline dimer is the α,ω-bis(4-(4-cyanophenyl)phenyloxy)alkanes [2]. This series

This work was partly supported by a Grant-in-Aid for Scientific Research from the Japan Society for the Promotion of Science (No. 19550175).

Address correspondence to Atsushi Yoshizawa, Department of Frontier Materials Chemistry, Graduate School of Science and Technology, Hirosaki Univesity, 3 Bunkyo-cho, Hirosaki 036-8561, Japan. E-mail: ayoshiza@cc.hirosaki-u.ac.jp

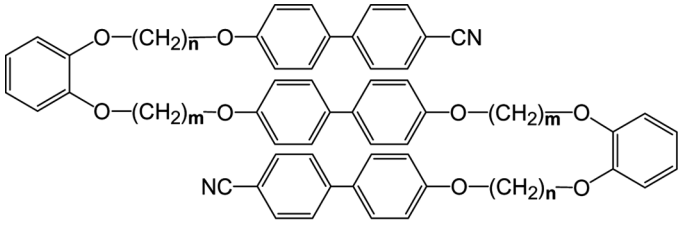

I-(m,n)

FIGURE 1 Molecular structure of the S-shaped liquid crystal oligomer.

exhibited a namatic (N) phase, and pronounced odd-even effects associated with spacer length were observed for their melting and nematic-isotropic transition temperatures. These dependences could be explained by using zig-zag shape for the even-numbered dimer and bent shape for odd-numbered dimer. Then, trimer [3] and tetramer [4] have ever been reported.

We have designed novel preorganized systems, e.g., a flexible dimesogenic compound [5], a U-shaped molecule [6], a binaphthyl derivative [7], a λ-shaped molecule [8], V-shaped [9], T-shaped [10] and Y-shaped molecules [11]; the preorganized supermolecules were found to induce unusual ordering in the supramolecular liquid crystalline phase. Recently, we reported pronounced odd-even effects in the transition behavior of U-shaped systems [12]. Moreover, we have reported the synthesis and transition properties of S-shaped molecules in which two U-shaped mesogenic molecules are connected [13].

For the present study, we prepared a homologous series of 4,4′-bis(ω-(2-(ω-(4-(cyanophenyl)phenyloxy)alkyloxy)phenyloxy)alkyloxy)-biphenyl [**I-(m,n)**] and investigated effects of spacer length on their liquid-crystalline properties. Figure 1 shows molecular structure of the S-shaped liquid-crystalline oligomer. We discuss packing and conformation for the S-shaped oligomers in their liquid crystalline phases.

2. EXPERIMENTAL

2.1. Preparation of Materials

Purification of the final products was carried out using HPLC (Japan Analytical Industry Co., Ltd., LC-9101, JAIGEL-2H column); chloroform was used as eluant. Detection of products was achieved by UV irradiation ($\lambda = 254$ nm). Recrystallization from ethanol gave the final products. Structures were elucidated using infrared (IR) spectroscopy (FTS-30; Bio Red Laboratories, Inc.) and proton nuclear magnetic resonance

spectroscopy (JMN-GX270; JOEL, JMN-A400; JOEL, or JMN-ECA500; JPEL). The analyses of the structures of the products by spectroscopic methods were found to be consistent with the predicted structures.

2.1.1. *4,4′-Bis(8-(2-(8-(4-(cyanophenyl)phenyloxy) octyloxy)phenyloxy)octyloxy)biphenyl, I-(8,8)*

Potassium carbonate (2.41 g, 17.5 mmol) was added to a solution of 4-cyano-4′-hydroxybiphenyl (2.92 g, 15 mmol) and 1,8-dibromohexane (5.40 g, 20 mmol) in cyclohexanone (45 mmol). The resulting mixture was stirred at 70°C for 10 h. After filtration of the precipitate, the solvent was removed by evaporation. The residue was purified by column chromatography on silica gel with toluene. Recrystallization from ethanol gave 4-cyano-4′-(8-bromooctyloxy)biphenyl; yield 2.93 g (51 %).

Potassium carbonate (0.69 g, 5.0 mmol) was added to a solution of 4-cyano-4′-(8-bromooctyloxy)biphenyl (1.93 g, 5.0 mmol) and 1,2-dihydroxybenzene (1.65 g, 15 mmol) in cyclohexanone (15 ml). The resulting mixture was stirred at 70°C for 11 h. After filtration of the precipitate, the solvent was removed by evaporation. The residue was purified by column chromatography on silica gel with dichloromethane. Recrystallization from ethanol gave 2-(8-(4-(cyanophenyl)-phenyloxy)octyloxy)phenol; yield 2.93 g (51%).

Potassium carbonate (1.74 g, 12.5 mmol) was added to a solution of 4,4′-dihydroxybiphenyl (1.86 g, 10 mmol) and 1,8-dibromooctane (10.95 g, 40 mmol) in acetone (50 ml). The resulting mixture was stirred under reflux for 12 h. After filtration of the precipitate, the solvent was removed by evaporation. The residue was reprecipitated with a mixture of chloroform and ethanol to give 4,4′-bis(8-bromooctybromooctyloxy)biphenyl; yield 1.40 g (25%).

Potassium carbonate (0.14 g, 1.0 mmol) was added to a solution of 2-(8-(4-(cyanophenyl)phenyloxy)octyloxy)phenol (0.42 g, 1.0 mmol) and 4,4′-bis(8-bromooctyloxy)biphenyl (0.23 g, 0.50 mmol) in cyclohexanone (10 ml). The resulting mixture was stirred at 120°C for 10 h. After filtration of the precipitate, the solvent was removed by evaporation. The residue was washed with dichloromethane and purified using HPLC with chloroform as eluant. Recrystallization from ethanol gave the desired product; yield 90 mg (14%).

^{1}H NMR (500 MHz, solvent $CDCl_3$, standard TMS) δ_H/ppm: 7.67 (d, 4H, Ar–**H**, $J = 8.6$ Hz), 7.62 (d, 4H, Ar–**H**, $J = 8.55$ Hz), 7.50 (d, 4H, Ar–**H**, $J = 8.55$ Hz), 7.43 (d, 4H, Ar–**H**, $J = 8.6$ Hz), 6.97 (d, 4H, Ar–**H**, $J = 9.2$ Hz), 6.92 (d, 4H, Ar–**H**, $J = 8.55$ Hz), 6.89–6.87 (m, 8H, Ar–**H**), 4.01–3.95 (m, 16H, Ar–O**CH_2**–). 1.86–1.74 (m, 16H, aliphatic–**H**). 1.53–1.45 (m, 16H, aliphatic–**H**). 1.43–1.36 (m, 16H, aliphatic–**H**). IR (KBr) ν/cm^{-1}: 2936, 2856 (C–H), 2224 (C≡N), 1602, 1497 (C=C).

The other compounds presented in this paper were obtained by a similar method to that for **I-(8,8)**. Analytical data for other compounds are given below.

2.1.2. *4,4′-Bis(9-(2-(9-(4-(cyanophenyl)phenyloxy) nonyloxy)phenyloxy)nonyloxy)biphenyl, I-(9,9)*

^{1}H NMR (500 MHz, solvent $CDCl_3$, standard TMS) δ_H/ppm: 7.67 (d, 4H, Ar–**H**, $J = 8.6$ Hz), 7.62 (d, 4H, Ar–**H**, $J = 8.6$ Hz), 7.50 (d, 4H, Ar–**H**, $J = 9.15$ Hz), 7.43 (d, 4H, Ar–**H**, $J = 9.15$ Hz), 6.97 (d, 4H, Ar–**H**, $J =$ 9.16 Hz), 6.92 (d, 4H, Ar–**H**, $J = 8.59$ Hz), 6.88 (m, 8H, Ar–**H**, $J = 8.59$ Hz), 4.02–3.94 (m, 16H, Ar–OC**H$_2$**–), 1.86–1.75 (m, 16H, aliphatic–**H**), 1.52–1.43 (m, 16H, aliphatic–**H**), 1.42–1.32 (m, 24H, aliphatic–**H**). IR (KBr) ν/cm^{-1}: 2928, 2852 (C–H), 2227 (C≡N), 1603, 1507 (C=C).

2.1.3. *4,4′-Bis(6-(2-(9-(4-(cyanophenyl)phenyloxy)nonyloxy) phenyloxy)hexyloxy)biphenyl, I-(6,9)*

^{1}H NMR (500 MHz, solvent $CDCl_3$, standard TMS) δ_H/ppm: 7.67 (d, 4H, Ar–**H**, $J = 7.45$ Hz), 7.62 (d, 4H, Ar–**H**, $J = 8.05$ Hz), 7.50 (d, 4H, Ar–**H**, $J = 8.55$ Hz), 7.43 (d, 4H, Ar–**H**, $J = 8.05$ Hz), 6.97 (d, 4H, Ar–**H**, $J = 8.6$ Hz), 6.92 (d, 4H, Ar–**H**, $J = 8.6$ Hz), 6.87 (m, 8H, Ar–**H**), 4.05–3.95 (m, 16H, Ar–OC**H$_2$**–), 1.91–1.76 (m, 16H, aliphatic–**H**), 1.62–1.53 (m, 8H, aliphatic–**H**), 1.52–1.43 (m, 8H, aliphatic–**H**), 1.42–1.31 (m, 12H, aliphatic–**H**). IR (KBr) ν/cm^{-1}: 2937, 2855 (C–H), 2227 (C≡N), 1603, 1507 (C=C).

2.1.4. *4,4′-Bis(7-(2-(9-(4-(cyanophenyl)phenyloxy) nonyloxy)phenyloxy)hepyloxy)biphenyl, I-(7,9)*

^{1}H NMR (500 MHz, solvent $CDCl_3$, standard TMS) δ_H/ppm: 7.67 (d, 4H, Ar–**H**, $J = 8.6$ Hz), 7.62 (d, 4H, Ar–**H**, $J = 8.6$ Hz), 7.50 (d, 4H, Ar–**H**, $J = 8.55$ Hz), 7.43 (d, 4H, Ar–**H**, $J = 9.2$ Hz), 6.97 (d, 4H, Ar–**H**, $J = 8.6$ Hz), 6.92 (d, 4H, Ar–**H**, $J = 9.15$ Hz), 6.89 (m, 8H, Ar–**H**), 4.04–3.95 (m, 16H, Ar–OC**H$_2$**–), 1.88–1.76 (m, 16H, aliphatic–**H**), 1.55–1.42 (m, 20H, aliphatic–**H**), 1.42–1.32 (m, 12H, aliphatic–**H**). IR (KBr) ν/cm^{-1}: 2934, 2854 (C–H), 2226 (C≡N), 1603, 1500 (C=C).

2.1.5. *4,4′-Bis(6-(2-(6-(4-(cyanophenyl)phenyloxy) hexyloxy)phenyloxy)hexyloxy)biphenyl, I-(6,6)*

^{1}H NMR (270 MHz, solvent $CDCl_3$, standard TMS) δ_H/ppm: 7.65 (d, 4H, Ar–**H**, $J = 8.6$ Hz), 7.59 (d, 4H, Ar–**H**, $J = 8.9$ Hz), 7.48 (d, 4H, Ar–**H**, $J = 8.9$ Hz), 7.41 (d, 4H, Ar–**H**, $J = 8.4$ Hz), 6.97–6.88 (m, 16H, Ar–**H**), 4.04–3.94 (m, 16H, Ar–OC**H$_2$**–), 1.85–1.52 (m, 12H, aliphatic–**H**). IR (KBr) ν/cm^{-1}: 2940, 2861 (C–H), 2224 (C≡N), 1601, 1498 (C=C).

2.1.6. *4,4′-Bis(7-(2-(7-(4-(cyanophenyl)phenyloxy) heptyloxy)phenyloxy)heptyloxy)biphenyl, I-(7,7)*

^{1}H NMR (400 MHz, solvent $CDCl_3$, standard TMS) δ_H/ppm: 7.66 (d, 4H, Ar–**H**, $J = 8.3$ Hz), 7.60 (d, 4H, Ar–**H**, $J = 8.3$ Hz), 7.49 (d, 4H, Ar–**H**, $J = 8.3$ Hz), 7.42 (d, 4H, Ar–**H**, 8.8 Hz), 6.97–6.89 (m, 16H, Ar–**H**), 4.02–3.95 (m, 16H, Ar–O**CH_2**–), 1.85–1.52 (m, 40H, aliphatic–**H**). IR (KBr) ν/cm^{-1}: 2947, 2856 (C–H), 2225 (C≡N), 1602, 1499 (C=C).

2.2. Liquid-Crystalline and Physical Properties

The initial phase assignments and corresponding transition temperatures for the final products were determined by optical polarized light microscopy using a Nikon Optiphot-pol polarizing microscope equipped with a Mettler FP82 hot stage and FP90 control processor. The heating and cooling rates were 5°C min^{-1}. The photomicrographs were taken using a camera (OLYMPUS DIGITAL CAMERA C-5050 ZOOM) in conjunction with a Nikon Optiphot-pol polarizing microscope. Temperatures and enthalpies of transition were investigated by differential scanning calorimetry (DSC) using a Seiko DSC6200 calorimeter. The compounds were studied at a scanning rate of 5°C min^{-1}, for both heating and cooling cycles, after being encapsulated in aluminium pans. X-ray diffraction patterns of the sample on cooling process were obtained using a real-time X-ray diffractometer (D8 Discover; Bruker AXS GmbH) equipped with a hot stage and a temperature-control processor. A sample was put on a convex lens, which was placed in a custum-made temperature stabilized holder (stability within ±0.1°C). The X-ray apparatus was equipped with a cross-coupled Göbel mirror on a platform system with a two-dimensional position-sensitive proportional counter (PSPC) detector (HI-Star; Bruker AXS GmbH). X-rays were generated at 40 kV and 40 mA; a parallel Cu Kα X-ray beam was used to irradiate the sample. Each diffraction pattern was obtained using the PSPC detector at a camera distance of 150 mm for a short counting time of 30 s.

2.3. Molecular Shape

Figure 2 shows MM2 models for **I-(m,n)** based on the assumption that intramolecular interactions between the cyanobiphenyl and biphenyl moieties cause the molecules to form a close-packed structure. Although a structure of a mesogenic molecule based on the MM2 calculation does not reflect the real conformation in the liquid-crystalline phase, the structure can give some information to discuss the observed structure-property relationships.

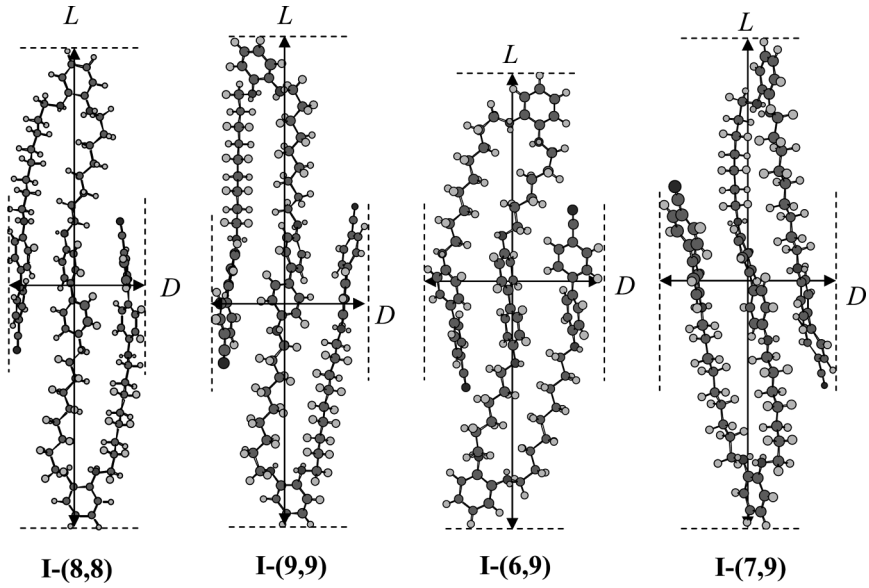

FIGURE 2 MM2 models for **I-(m,n)**.

3. RESULTS AND DISCUSSION

3.1. Phase Transion Properties

Transition temperatures and transition enthalpies for S-shaped liquid-crystalline oligomers **I-(m,n)** measured by optical polarized light microscopy and differential scanning calorimetry (DSC) are listed in

TABLE 1 Phase Transition Temperature (°C), Enthalpies (kJ mol^{-1}) of Transition (in Brackets) and Transition Entropies ($\Delta S/R$) for S-Shaped Compounds **I-(m,n)** on Cooling

Compound	Phase transition tmperatures/°C (ΔH/kJ mol^{-1})	$\Delta S_{\text{N-SmA}}/R$	$\Delta S_{\text{I-N}}/R$
I–(6,6)	Cr 154 [N 139 (0.71)] Iso		0.21
I–(7,7)	Cr 85 SmA 100 (3.38) N 105 (0.95) Iso	1.09	0.31
I–(8,8)	Cr 139 [SmA 115[a] N 132 (4.59)] Iso		1.36
I–(9,9)	Cr 89 SmA 107[b] N 108[b] Iso		
I–(6,9)	Cr 120 [N 119 (2.76)] Iso		0.85
I–(7,9)	Cr 82 SmA 97 (3.27) N 102 (1.11) Iso	1.07	0.35

[a]The N-SmA transition enthalpy was too small to be detected.
[b]The Iso-N and N-SmA transitions occurred simultaneously. The total value of both transition enthalpies was 11.2 kJ mol^{-1}.

Table 1. Compounds **I-(6,6)** and **I-(6,9)** exhibited a nematic (N) phase, whereas compounds **I-(7,7), I-(8,8), I-(9,9)**, and **I-(7,9)** exhibited nematic and smectic A (SmA) phases. Pronounced odd-even effects were observed for the Iso-N and N-SmA transition temperatures of the S-shaped oligomers as the parity of the spacer was varied.

The melting behavior was found to depend on the parity of the spacer. DSC thermograms for **I-(6,6)** and **I-(7,7)** are shown in Figure 3. Compound **I-(6,6)** showed a Cry to Iso transition at 154°C, and exhibited a monotropic N phase on cooling. There is marked hysteresis in phase transition behavior between heating and cooling processes of compound **I-(6,6)**. On the other hand, there is no significant difference in transition behavior between heating and cooling processes of compound **I-(7,7)**. DSC measurements of all the compounds revealed that the melting behavior depends on the parity (m) of the spacer. Lower melting temperatures for compounds **I-(7,7), I-(9,9)**

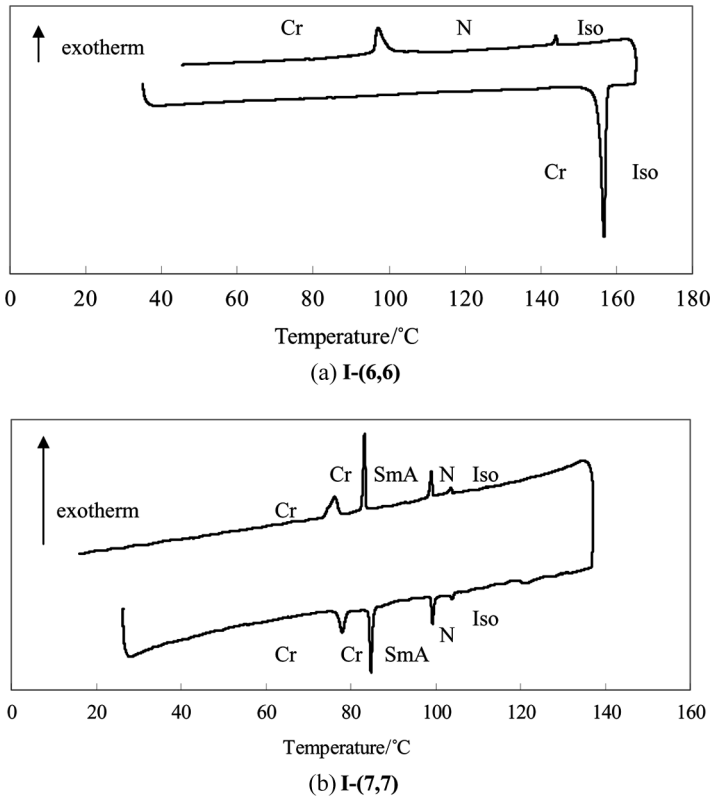

FIGURE 3 DSC thermograms for (a) **I-(8,8)** and (b) **I-(7,7)**.

and **I-(7,9)** are thought to be attributed to loose molecular packing in the crystalline phases.

We compared the transition properties of **I-(8,8)** with those of **I-(7,7)**. Both compounds exhibited a phase sequence of Iso-N-SmA. Their transition entropies ($\Delta S/R$) are listed in Table 1. Surprisingly, the associated entropy change at the N–SmA transition of **I-(8,8)** was negligible small. The associated entropy change at the Iso-N transition of **I-(8,8)** was almost corresponding to the total value of both the I-N and N-SmA transition entropies of **I-(7,7)**. The results suggested a possibility that the N phase of **I-(8,8)** has a smectic-like layer ordering. We will discuss it later.

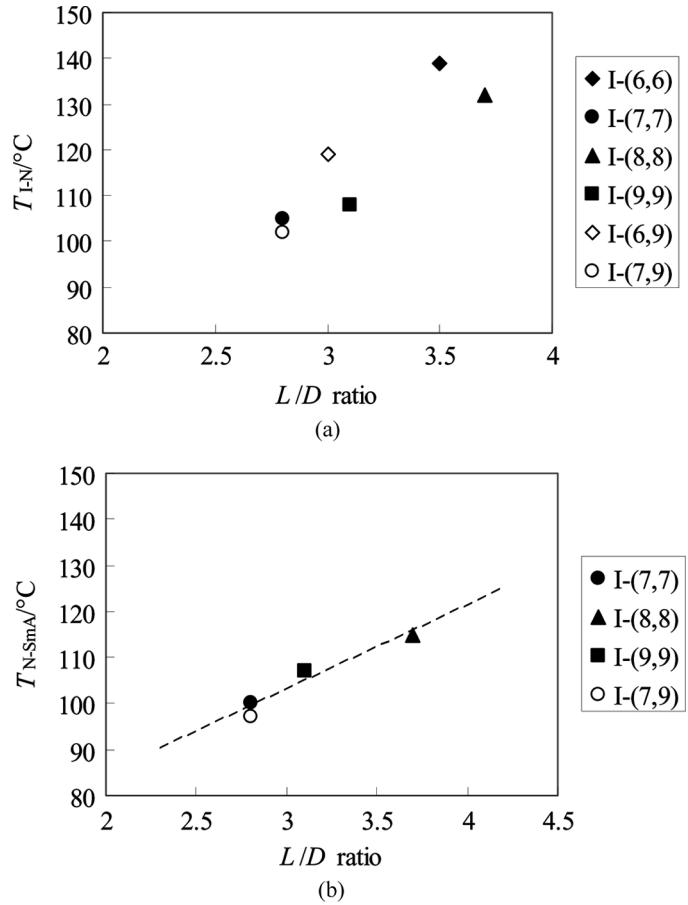

FIGURE 4 (a) Relationship between $T_{I\text{-}N}$ and L/D ratio for compound **I-(m,n)**. (b) Relationship between $T_{N\text{-}SmA}$ and L/D ratio for compound **I-(m,n)**.

3.2. Relationship Between Molecular Shape and Transition Temperature

Isotropic-nematic transition temperature ($T_{I\text{-}N}$) is plotted against L/D for the S-shaped oligomers in Figure 4(a). As increasing L/D ratio, $T_{I\text{-}N}$

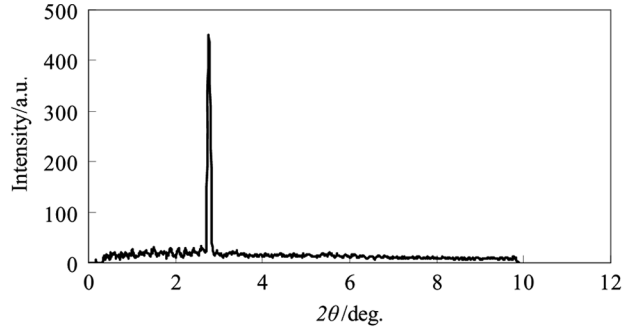

(a) **I-(7,7)** (93°C)

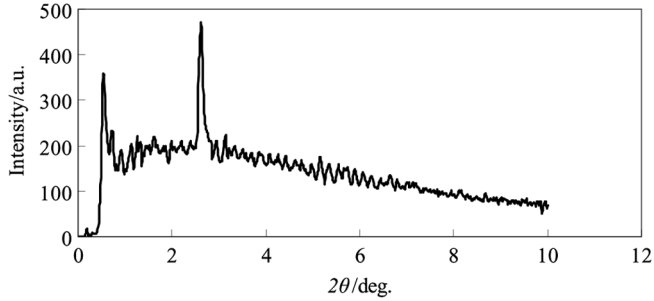

(b) **I-(8,8)** (110°C)

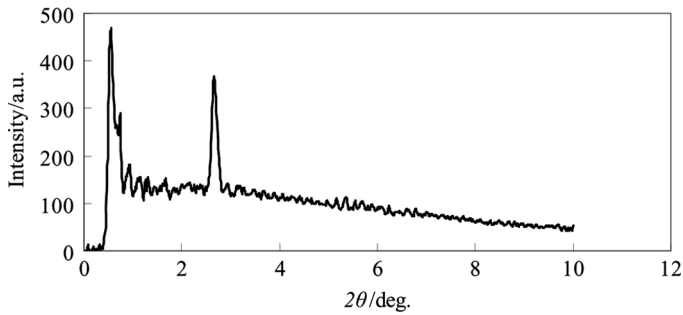

(c) **I-(7,9)** (90°C)

FIGURE 5 X-ray diffraction patterns in the SmA phase of (a) **I-(7,7)**, (b) **I-(8,8)** and (c) **I-(7,9)**.

TABLE 2 Molecular Length (l) and Layer Spacing (d) in the SmA Phase of **I-(m,n)**

Compound	l^a/Å	d^b/Å
I–(7,7)	35	32
I–(8,8)	39	34
I–(7,9)	35	33

[a]The estimated molecular length from MM2 calculation.
[b]The layer spacing obtained from X-ray diffraction measurements.

increases. Therefore, the excluded volume effects due to molecular shape promote formation of the N phase. Figure 4(b) shows relationship between namatic-smectic A transition temperature ($T_{\text{N-SmA}}$) and L/D ratio. There is good linearity between them. Compounds with even-membered (m) spacers have larger L/D ratio than those with odd-membered (m) spacers. The odd-even effects for the Iso-N and N-SmA transition temperatures of the S-shaped oligomers are explainable in terms of L/D ratio. However, $T_{\text{N-SmA}}/(L/D)$ is smaller than $T_{\text{I-N}}/(L/D)$. Not only the excluded volume effect but also an electrostatic interaction plays an important role in formation of the SmA phase.

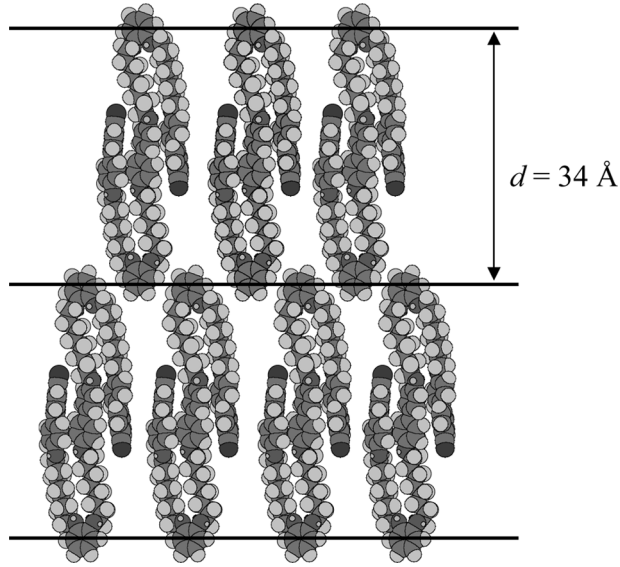

FIGURE 6 Possible model of the molecular organization in the SmA phase of **I-(8,8)**.

3.3. X-ray Diffraction Studies

Figure 5 shows X-ray diffraction patterns in the small angle region in the SmA phase of (a) **I-(7,7)**, (b) **I-(8,8)** and (c) **I-(7,9)**. The estimated molecular length (l) from MM2 calculation and the layer spacing (d) obtained from the XRD measurements are summarized in Table 2. Although $\Delta S/R$ at the N-SmA transition for **I-(8,8)** is negligible small, XRD studies indicate that there is no significant positional order in the N phase of **I-(8,8)**. The obtained layer spacings of the SmA phase for **I-(7,7), I-(8,8)**, and **I-(7,9)** were about 32, 34, and 33 Å, respectively. Figure 6 shows a possible model for molecular organization in the SmA phase of **I-(8,8)**. The model suggests that: (1) the oligomer forms a close-packed S-shaped structure, (2) antiparallel interactions between neighboring cyanobiphenyl groups exist in each layer, and 3) interlayer interactions between the phenyl units occur.

4. CONCLUSIONS

We prepared a homologous series of S-shaped oligomers and investigated their phase transition behavior. All S-shaped oligpmers exhibited an N phase. In addition, compounds **I-(7,7), I-(8,8), I-(9,9)**, and **I-(7,9)** also exhibited an SmA phase. Pronounced odd-even effects were observed for melting behavior, $T_{\text{I-N}}$ and $T_{\text{N-SmA}}$ of the S-shaped oligomers. Furthermore, XRD measurements indicate that the SmA phase has a monolayer structure composed of the close-packed S-shaped oligomers.

REFERENCES

[1] (a) Goodby, J. W., Mehl, G. H., Saez, I. M., Tuffin, R. P., Mackenzie, G., Auzely-Velty, R., Benvegu, T., & Plusquellec, D. (1998). *Chem. Commun.*, 2057; (b) Saez, I. & Goodby, J. W. (2005). *J. Mater. Chem.*, *15*, 26.

[2] (a) Emsley, J. W., Luckhurst, G. R., Shilstone, G. N., & Sage, I. (1984). *Mol. Cryst. Liq. Cryst.*, *102*, 223; (b) Luckhurst, G. R. (2005). *Liq. Cryst.*, *32*, 1335.

[3] (a)Tsvetkov, N. V., Zuev, V. V., & Tsvetkov, V. N. (1997). *Liq. Cryst.*, *22*, 245; (b) Henderson, P. A., Cook, A. G., & Imrie, C. T. (2004). *Liq. Cryst.*, *31*, 1427.

[4] (a) Imrie, C. T., Stewart, D., Remy, C., Christie, D. W., Hamley, I. W., & Harding, R. (1999). *J. Mater. Chem.*, *9*, 2321; (b) Henderson, P. A. & Imrie, C. T. (2005). *Liq. Cryst.*, *32*, 673.

[5] (a) Yoshizawa, A., Ise, N., & Okada, T. (1998). *Ferroelectrics*, *213*, 75; (b) Yoshizawa, A., Yamamoto, K., Dewa, H., Nishiyama, I., & Yokoyama, H. (2003). *J. Mater. Chem.*, *13*, 172; (c) Yoshizawa, A., Kurauchi, M., Kohama, M., Dewa, H., Yamamoto, K., Nishiyama, I., Yamamoto, T., Yamamoto, J., & Yokoyama, H. (2006). *Liq Cryst.*, *33*, 611.

[6] Yoshizawa, A. & Yamaguchi, A. (2002). *Chem. Commun.*, 2060.

[7] (a)Rokunohe, J. & Yoshizawa, A. (2005). *J. Mater. Chem.*, *15*, 275; (b) Rokunohe, J., Yamaguchi, A., & Yoshizawa, A. (2005). *Liq. Cryst.*, *32*, 207.

[8] Yamaguchi, A., Nishiyama, I., Yamamoto, J., Yokoyama, H., & Yoshizawa, A. (2005). *Mol. Cryst. Liq. Cryst.*, *439*, 85.
[9] Yoshizawa, A., Kinbara, H., Narumi, T., Yamaguchi, A., & Dewa, H. (2005). *Liq. Cryst.*, *32*, 1175.
[10] Yoshizawa, A., Sato, M., & Rokunohe, J. (2005). *J. Mater. Chem.*, *15*, 3285.
[11] Yoshizawa, A., Nakata, M., & Yamaguchi, A. (2006). *Liq. Cryst.*, *33*, 605.
[12] Yamaguchi, A., Watanabe, M., & Yoshizawa, A. (2007). *Liq. Cryst.*, *34*, 633.
[13] Yoshizawa, A., Kasai, H., Ogasawara, F., Nagashima, Y., & Kawaguchi, T. (2007). *Liq. Cryst.*, *34*, 547.